JOURNAL OF MATERIALS SCIENCE 37 (2002) 335–342

Densification and microstructural developments during the sintering of aluminium silicon carbide

K. ITATANI*, F. TAKAHASHI, M. AIZAWA, I. OKADA
Department of Chemistry, Faculty of Science and Engineering, Sophia University, 7-1 Kioi-cho, Chiyoda-ku, Tokyo 102-8554, Japan
E-mail: itatani@sophia.ac.jp

I. J. DAVIES
Advanced Fibro-Science, Kyoto Institute of Technology, Matsugasaki, Sakyo-ku, Kyoto 606-8585, Japan

H. SUEMASU, A. NOZUE
Department of Mechanical Engineering, Faculty of Science and Engineering, Sophia University, 7-1 Kioi-cho, Chiyoda-ku, Tokyo 102-8554, Japan

Densification and microstructural developments during the sintering of aluminum silicon carbide (Al_4SiC_4) were examined. Two types of Al_4SiC_4 powders were prepared by the solid-state reactions between: (i) Al, Si, and C at 1600°C for 10 h (designated as Al_4SiC_4(SSR)), and (ii) chemically-vapour deposited ultrafine Al_4C_3 and SiC powders at 1500°C for 4 h (Al_4SiC_4(CVD/SSR)). The specific surface areas of the Al_4SiC_4(SSR) and Al_4SiC_4(CVD/SSR) powders were 2.7 and 15.5 $m^2 \cdot g^{-1}$, respectively. Relative densities of the pressureless-sintered Al_4SiC_4(SSR) and Al_4SiC_4(CVD/SSR) compacts were as low as 60–70% for firing temperatures between 1700°C and 2000°C. The relative densities of Al_4SiC_4(SSR) and Al_4SiC_4(CVD/SSR) compacts could be enhanced using the hot-pressing technique; the relative density of the Al_4SiC_4(SSR) compact hot-pressed at 1900°C for 3 h was 97.0% whereas that of the Al_4SiC_4(CVD/SSR) compact hot-pressed at 1900°C for 1 h attained 99.0%. The former microstructure was composed of plate-like grains of width 10–30 μm and thickness ~10 μm whilst the latter microstructure was comprised of equiaxed grains with a typical diameter of ~10 μm. Densification of the Al_4SiC_4(CVD/SSR) compacts appeared to be promoted compared to the Al_4SiC_4(SSR) compact and this was attributed to the higher surface area, reduced agglomeration of the starting primary particles, and more homogeneous chemical composition.

1. Introduction

The existence of aluminum silicon carbide (Al_4SiC_4), together with optical and X-ray powder diffraction data, was first reported by Barczak [1] whilst Schoennahl *et al*. [2] later clarified thermal, chemical, and mechanical properties. Since that time, several researchers have paid attention to the thermal stability of Al_4SiC_4 formed during either a blast furnace process or the carbothermal reduction of bauxite or clay minerals, with regards to the production of low-cost aluminium [3–5].

Sintered Al_4SiC_4 compacts possess higher compressive strength (~260 GPa) compared to that of SiC (~165 GPa) [2] and also exhibit potential as a high toughness material due to the possibility of microcrack deflection along the plate-like grains formed during firing [3]. In addition to this, Al_4SiC_4 has also been used as a sintering aid for silicon carbide (SiC) [2].

Al_4SiC_4 starting powder has generally been prepared by solid state reactions between Al, Si, and C [1, 4] or else Al_4C_3 and SiC [6]. The present authors have prepared ultrafine Al_4C_3 and SiC powders using the chemical vapour deposition (CVD) technique [7, 8], leading to the formation of Al_4SiC_4 powder at a temperature as low as 1500°C [8].

Although, generally speaking, dense ceramics may be fabricated when the powder is consolidated without entrapping pores within the grains, many additional factors also exist that affect the sinterability of ceramic powder. For example, the effect of oxygen impurity on the sintering behaviour of Al_4SiC_4 powder has been examined by Oscroft and Thompson [9], who pointed out that oxygen within the Al_4SiC_4 powder promotes the formation of liquid aluminosilicate phases above 1700°C, thereby accelerating densification. However, no additional factors that affect the sinterability of Al_4SiC_4 powder have been examined thus far. In the present work, the authors prepared two types of Al_4SiC_4 powders and examined the effect of powder properties

*Author to whom all correspondence should be addressed.

on the densification and microstructural development of Al_4SiC_4 using pressureless sintering and hot pressing techniques.

2. Experimental procedure

2.1. Preparation of the starting Al_4SiC_4 powders

Two kinds of Al_4SiC_4 powders were prepared by the solid state reactions between: (i) Al, Si, and C (designated as Al_4SiC_4(SSR)), and (ii) chemically vapour deposited ultrafine Al_4C_3 and SiC powders (Al_4SiC_4 (CVD/SSR)). Preparation conditions for the Al_4SiC_4 powders were as follows:

The Al_4SiC_4(SSR) starting powder was prepared by mixing stoichiometric amounts of Al (>99.5% purity), Si (99.9% purity), and C (activated charcoal) powders (Wako Pure Chemicals, Tokyo, Japan) in the presence of *n*-hexane using a zirconia mortar and pestle. The resulting powder mixture was heated at 1600°C for 10 h in an argon (Ar) atmosphere to result in the Al_4SiC_4 powder.

The Al_4SiC_4(CVD/SSR) starting powder was prepared by mixing ultrafine Al_4C_3 and SiC powders (prepared by the chemical vapour deposition of trimethylaluminum ($Al(CH_3)_3$) and triethylsilane ($SiH(C_2H_5)_3$) at 1000°C, respectively) in the presence of *n*-hexane and followed by heating at 1500°C for 4 h in an Ar atmosphere to result in the Al_4SiC_4 powder.

2.2. Pressureless sintering and hot pressing of the powder compacts

Two types of powder compact were fabricated using the following procedures: (i) approximately 0.2 g of powder was uniaxially pressed at 100 MPa in order to form a compact with a diameter and thickness of 10 mm and ~2 mm, respectively, and (ii) approximately 2.0 g of powder was pressed at 100 MPa to form a compact with a diameter and thickness of 19 mm and ~3 mm, respectively. The former compact was used for the pressureless sintering procedure whereas the latter was employed for hot pressing. In the case of pressureless sintering, the compact was embedded in Al_4SiC_4 powder in order to suppress thermal decomposition whilst, for the case of hot pressing, the compact was uniaxially pressed in a graphite die at 31 MPa. The pressureless sintering and hot pressing procedures were conducted at temperatures between 1700°C and 2000°C in an Ar atmosphere and furnace cooled.

2.3. Evaluation

The particle morphologies were observed using a scanning electron microscope (SEM; Model S-4500, Hitachi, Tokyo, Japan; accelerating voltage 5 kV) and transmission electron microscope (TEM; Model H-300, Hitachi, Tokyo; accelerating voltage 100 kV). The oxygen content of the starting powder was checked using a wavelength-dispersive X-ray microanalyser (WDX) attached to an electron probe microanalyser (Model JXA-8600SX, JEOL, Tokyo; accelerating voltage; 20 kV). Specific surface areas of the starting powders were measured using a BET technique and nitrogen (N_2) as an adsorption gas. Crystalline phases of the powders and sintered compacts were identified using an X-ray powder diffractometer (XRD; Model RINT-2000, Rigaku, Tokyo; 40 kV, 40 mA) and monochromated Cu Kα radiation whilst crystalline phases on and near the surfaces were examined using a thin-film XRD (TF-XRD). Semi-quantitative analysis of aluminium and silicon amounts in the sintered compacts was conducted using an energy-dispersive X-ray microanalyser (EDX; Model EMAX 5770, Kyoto; accelerating voltage 20 kV) attached to the SEM apparatus.

The relative density of the sintered compact was calculated from the percentage of bulk density and true density. Bulk density was calculated from the mass and dimensions of the sintered compact whereas the true density was measured picnometrically at 30.0°C after pulverizing the sintered compact. Fracture surfaces of the sintered compacts were observed using SEM whilst the polished surfaces of sintered compacts were examined following etching with Murakami reagent [10]. In addition to this, indentation tests were conducted on the polished surfaces of hot-pressed compacts using a microhardness tester (Model M-400 MUK-E, Akashi, Tokyo).

3. Results and discussion

3.1. Properties of the starting Al_4SiC_4 powders

The densification of a ceramic compact is known to be strongly affected by the properties of the starting powders. The typical properties for the present system are described in this section. The only crystalline phase detected by XRD in the powders was Al_4SiC_4.

Previous work by the authors indicated the oxygen content of the Al_4SiC_4(CVD/SSR) powder to be 1.25 mass% [8]. On the other hand, the oxygen content of the Al_4SiC_4(SSR) powder measured by WDX was 5.43 mass%. The oxygen content of the Al_4SiC_4(CVD/SSR) powder is significantly lower compared to that of Al_4SiC_4(SSR) powder.

SEM micrographs for the powders have been shown in Fig. 1, together with a typical TEM micrograph. The Al_4SiC_4(SSR) powder (Fig. 1a) was comprised of agglomerates with typical sizes in the range 5–30 μm. The agglomerates appeared to consist of strongly bonded primary particles with a size less than 1 μm. In contrast to this, the Al_4SiC_4(CVD/SSR) powder (Fig. 1b) was composed of equiaxed particles with diameters on the order of ~0.1 μm and weakly coagulated.

The specific surface area and average primary particle size of the Al_4SiC_4(SSR) powder were 2.7 $m^2 \cdot g^{-1}$ and 0.730 μm, respectively, whereas those of the Al_4SiC_4(CVD/SSR) powder were 15.5 $m^2 \cdot g^{-1}$ and 0.099 μm, respectively.

The particles observed by SEM and TEM correspond to the primary particles, as their sizes were similar to those of the primary particle sizes mentioned above. The primary particle size of the Al_4SiC_4(CVD/SSR) powder is significantly smaller and well dispersed compared to that of the Al_4SiC_4(SSR) powder.

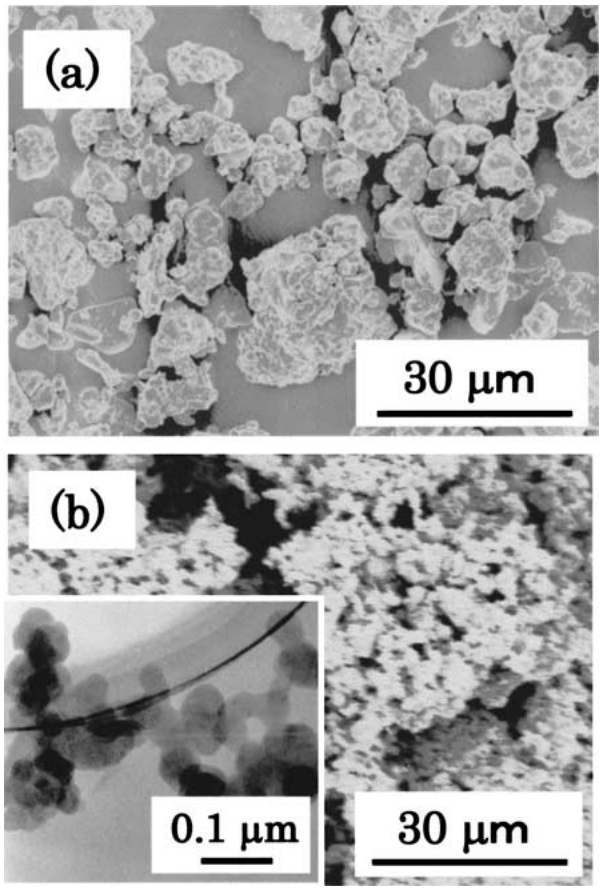

Figure 1 (a) SEM micrograph for Al_4SiC_4(SSR) powder, and (b) SEM and TEM micrographs for Al_4SiC_4 (CVD/SSR) powder.

3.2. Fabrication of dense Al_4SiC_4 compacts

3.2.1. Densification process of the Al_4SiC_4(SSR) powder compact

In this section, optimum conditions for the fabrication of dense Al_4SiC_4(SSR) compacts were examined using the pressureless sintering and hot pressing techniques. Fig. 2 shows the effect of sintering temperature on the relative density of the Al_4SiC_4(SSR) compact fabricated using the pressureless sintering and hot-pressing techniques. The relative densities of the pressureless-sintered Al_4SiC_4(SSR) compacts remained close to 60%, irrespective of the sintering temperature. In contrast to this, the relative density of the Al_4SiC_4(SSR) compact increased with hot pressing temperature to reach 92.6% at 2000°C.

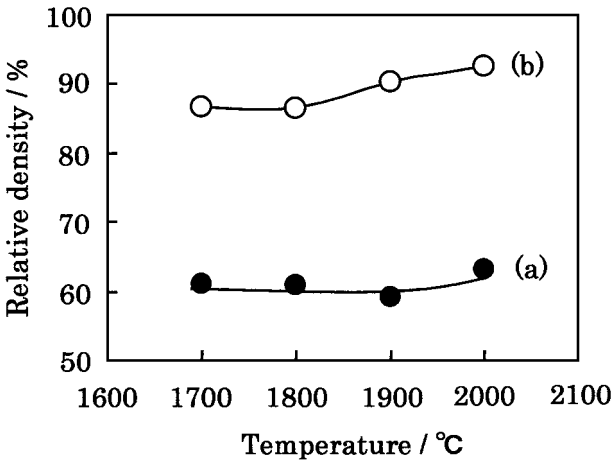

Figure 2 Effect of firing temperature on the relative densities of (a) pressureless-sintered, and (b) hot-pressed Al_4SiC_4(SSR) compacts. Note that the firing time was fixed to be 1 h for both cases.

Crystalline phases of the hot-pressed Al_4SiC_4(SSR) compacts were examined using XRD. Although not shown in this paper, the XRD pattern for the Al_4SiC_4(SSR) compact hot-pressed at 1800°C for 1 h showed the presence of only Al_4SiC_4 [11]. On the other hand, the Al_4SiC_4(SSR) compact hot-pressed at 1900°C for 1 h contained Al_4SiC_4 and α-SiC [12], whilst the Al_4SiC_4(SSR) compact hot-pressed at 2000°C for 1 h was composed of Al_4SiC_4, $Al_4Si_2C_5$ [13], and α-SiC.

As α-SiC was detected within the hot-pressed Al_4SiC_4(SSR) compact at 1900°C for 1 h, it is probable that a portion of the α-SiC was formed by the thermal decomposition of Al_4SiC_4: [14]

$$Al_4SiC_4 \rightarrow 4Al + SiC + 3C \qquad (1)$$

Although Al was not detected by XRD, this fact may be explained by assuming that the evaporation of Al during hot pressing makes detection difficult. The assumption of Al evaporation was further supported by the presence of metal-like deposits being noted on the surfaces of the hot-pressing dies. Referring to the evaporation of Al, the equilibrium vapor pressure of Al in the presence of Al_4SiC_4, SiC, and C between 1154°C and 1511°C can be expressed as follows: [14]

$$\log p = -(18567 \pm 86)(1/T) + (12.143 \pm 0.054) \qquad (2)$$

where p is the equilibrium vapour pressure (Pa) of Al and T is the absolute temperature (K). According to Equation 2, Al may easily evaporate from Al_4SiC_4. However, the evaporation of Al from Al_4SiC_4 should be avoided in order to fabricate dense Al_4SiC_4 (SSR) compacts. In the case of pressureless sintering, however, the decomposition appears to proceed, regardless of the Al_4SiC_4(SSR) compact being embedded in Al_4SiC_4 powder at 1700–2000°C. However, in the case of hot pressing, thermal decomposition may be suppressed, thereby leading to increased densification [9].

Moreover, the Al_4SiC_4(SSR) compact hot-pressed at 2000°C contained not only Al_4SiC_4 and α-SiC but also $Al_2Si_2C_5$. This $Al_4Si_2C_5$ may be formed on the basis of the following thermal decomposition of Al_4SiC_4:

$$2Al_4SiC_4 \rightarrow Al_4Si_2C_5 + 4Al + 3C \qquad (3)$$

The relative densities of hot-pressed Al_4SiC_4(SSR) compacts were significantly greater compared to the pressureless-sintered Al_4SiC_4(SSR) compacts. Densification of the Al_4SiC_4 compact during hot pressing may be promoted by the formation of aluminosilicate liquids without dissociation [9], chiefly due to the rearrangement of grains resulting in closer packing.

Since the relative density was limited to 92.6% at 2000°C, the effect of hot-pressing time on the densification of the Al_4SiC_4(SSR) compact was examined by fixing the hot pressing temperature to be 1900°C. This hot pressing temperature (1900°C) was selected in order to promote densification without appreciable thermal decomposition. Fig. 3 shows the effect of hot pressing time on the relative density and Vickers hardness of the

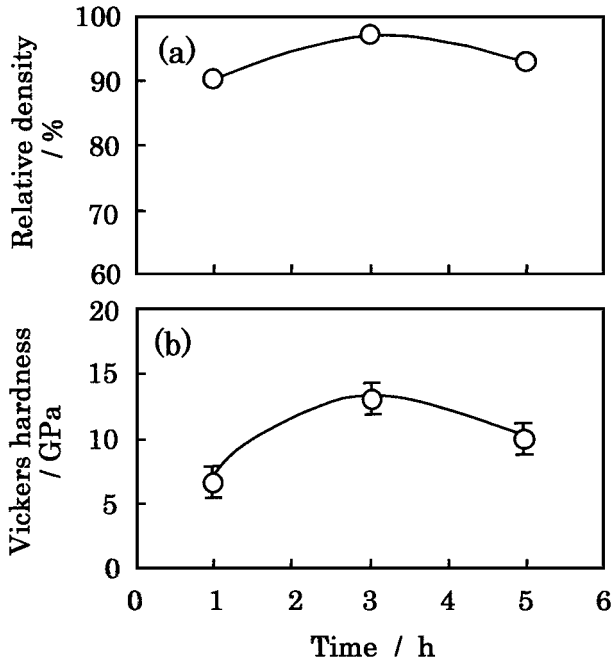

Figure 3 Effect of hot pressing time on the (a) relative density, and (b) Vickers hardness of Al_4SiC_4(SSR) compacts. Hot pressing temperature: 1900°C.

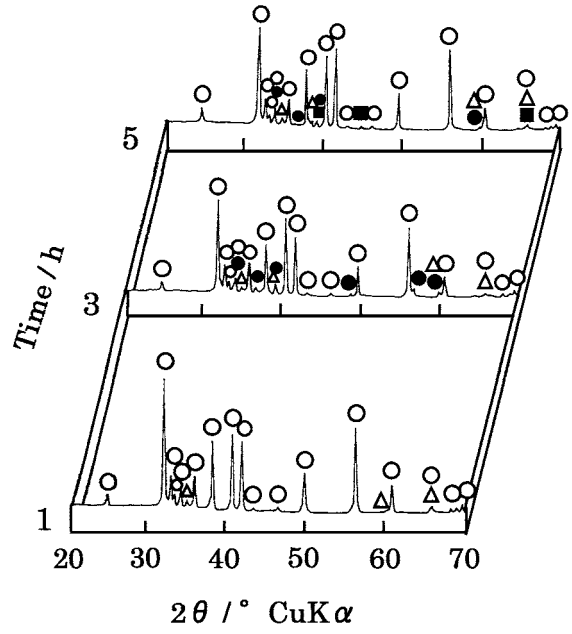

Figure 5 XRD patterns for Al_4SiC_4(SSR) compacts hot-pressed at 1900°C for 1 h, 3 h, and 5 h. ○: Al_4SiC_4 ●: $Al_4Si_2C_5$ ■: Al △: α-SiC.

Al_4SiC_4(SSR) compact. The relative density increased with hot pressing time and reached a value of 97.0% for the case of 3 h but then decreased to 92.7% for the case of 5 h. Reflecting the changes in relative density, Vickers hardness increased to a value of 13.1 GPa for the hot-pressing time of 3 h but then decreased upon further increases in hot pressing time.

The maximum Vickers hardness of 13.1 GPa agrees well with that reported previously [2] whilst the decrease in value for a hot-pressing time of 3 h to 5 h is attributed to the reduction of relative density and also to partial decomposition of Al_4SiC_4.

A typical SEM micrograph for the Al_4SiC_4(SSR) compact hot-pressed at 1900°C for 3 h is presented in Fig. 4 and indicates the presence of closely packed plate-like grains of width 10–30 μm and thickness ~10 μm. The closely-packed plate-like grains reflect the high relative density (97.0%). The densification of the Al_4SiC_4(SSR) compact may thus be associated with the formation of aluminosilicate liquids.

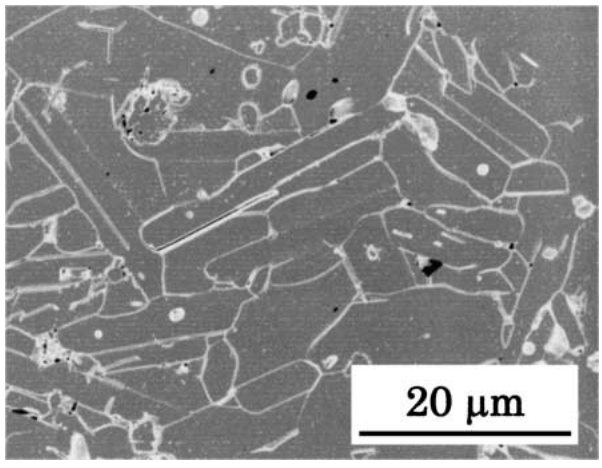

Figure 4 Typical SEM micrograph for an Al_4SiC_4(SSR) compact hot-pressed at 1900°C for 3 h. Note that the microstructure in the SEM micrograph was chemically etched using Murakami reagent [10].

In order to further understand the densification and Vickers hardness behaviour, the compacts were examined using XRD for the Al_4SiC_4(SSR) compact as a function of hot pressing duration at 1900°C. Typical XRD patterns are shown in Fig. 5 with all of the hot-pressed compacts containing Al_4SiC_4 as the major phase and a trace of α-SiC. The compacts hot-pressed for 3 h or more also contained $Al_4Si_2C_5$ and, furthermore, the compact hot-pressed for 5 h contained Al.

As mentioned previously, the relative density of the Al_4SiC_4(SSR) compact reached 97.0% for the hot-pressing time of 3 h and then reduced to 92.7% for 5 h. In addition, densification of the Al_4SiC_4(SSR) compact may be promoted by the closer packing of grains as a result of rearrangement due to the formation of liquid phases. Although the relative density of the Al_4SiC_4 compact decreased with hot-pressing time from 3 to 5 h, this phenomenon may be explained in terms of the creation of pores due to the thermal decomposition of Al_4SiC_4 to form $Al_4Si_2C_5$ and Al (see Equation 3). The creation of pores may also be confirmed by the fact that the Vickers hardness was reduced with hot-pressing time from 3 h to 5 h. The melting point of Al is 660°C and is therefore present as forms of vapour ⇋ liquid phases during hot pressing. Moreover, the aluminosilicates formed during pressureless sintering and hot pressing may change into liquid phases above 1700°C [9]. The liquid phases or vapour ⇋ liquid phases are known to promote anisotropic grain growth [3, 9], thereby changing the grain shape from equiaxed to plate-like. Regardless of such anisotropic grain growth, the closer packing of grains may be promoted by hot pressing, partly because the gas evolution due to liquid dissociation appears to be restricted by hot pressing [9], and partly because the aluminosilicates

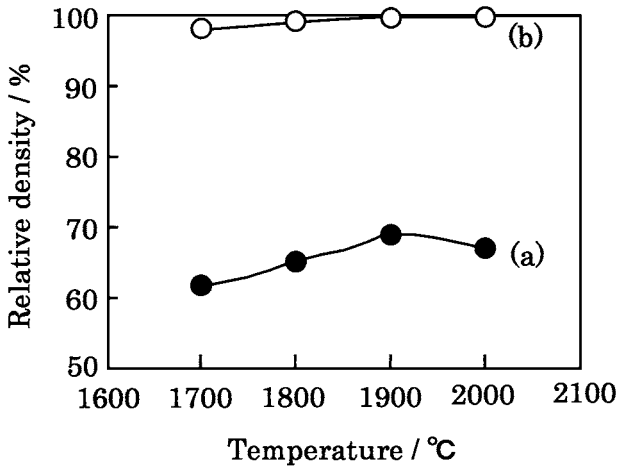

Figure 6 Effect of firing temperature on the relative densities of (a) pressureless-sintered and (b) hot-pressed Al_4SiC_4(CVD/SSR) compacts. Note that the firing time was fixed to be 1 h for both cases.

liquid phases formed above 1700°C help rearrangement of the grains toward closer packing.

3.2.2. Densification process of the Al_4SiC_4(CVD/SSR) compact

In this section, the fabrication conditions necessary for dense Al_4SiC_4(CVD/SSR) compacts will be examined. The effect of temperature on the relative density of Al_4SiC_4(CVD/SSR) compact has been presented in Fig. 6. The relative densities of pressureless-sintered Al_4SiC_4(CVD/SSR) compacts were in the range 60–70% for all sintering temperatures examined. On the other hand, the relative density of the Al_4SiC_4(CVD/SSR) compact increased with hot pressing temperature and reached 99.0% at 1900°C for 1 h. It is not surprising that the maximum density of the Al_4SiC_4(CVD/SSR) compact was greater than that of the Al_4SiC_4(SSR) compact if we consider the specific areas of the starting powders (15.5 and 2.7 $m^2 \cdot g^{-1}$, respectively).

The microstructures of pressureless-sintered and hot-pressed Al_4SiC_4(CVD/SSR) compacts were observed using SEM. Typical micrographs for the fracture surfaces (2000°C for 1 h) are shown in Fig. 7, together with the respective XRD patterns. The pressureless-sintered Al_4SiC_4(CVD/SSR) compact (Fig. 7a) contained randomly arranged plate-like grains of width 30–50 μm and thickness ~10 μm together with a large amount of porosity. The XRD pattern showed the presence of Al_4SiC_4 and α-SiC. The Al_4SiC_4 was present with the (110) reflection being very intense in comparison with that of the respective JCPDS card [11] (Fig. 7a'). In comparison to this, the hot-pressed Al_4SiC_4(CVD/SSR) compact (Fig. 7b) contained closely packed equiaxed grains with diameters of ~10 μm. The XRD result showed Al_4SiC_4 to be the major phase with $Al_4Si_2C_5$ and α-SiC being present as minor phases (Fig. 7b').

Although the relative densities of the pressureless-sintered Al_4SiC_4(CVD/SSR) compacts were in the range 60–70%, such low values may be attributed to anisotropic grain growth appearing to occur in both the a- and b-axis directions of the Al_4SiC_4 crystals, judging from the fact that the (110) reflection was intense in comparison with that of the respective JCPDS card. On the other hand, the relative density of the Al_4SiC_4(CVD/SSR) compact hot-pressed at 1900°C for 1 h was 99.0% and greater than the maximum relative density (97.0%) for the hot-pressed Al_4SiC_4(SSR) compacts. This phenomenon may be explained in terms of the higher specific surface area (15.5 $m^2 \cdot g^{-1}$) and reduced agglomeration of the Al_4SiC_4(CVD/SSR) powder compared to the case of Al_4SiC_4(SSR) powder. Note that the Al_4SiC_4(CVD/SSR) compact grain morphology pressureless-sintered at 2000°C for 1 h was plate-like whereas that of the Al_4SiC_4(CVD/SSR) compact hot-pressed at 2000°C for 1 h was equiaxed, suggesting the amount of aluminosilicate liquids present in the Al_4SiC_4(CVD/SSR) case to be insufficient to promote anisotropic grain growth. Moreover, the thermal decomposition of Al_4SiC_4 in the Al_4SiC_4(CVD/SSR) compact appears to be restricted, compared to that in the Al_4SiC_4(SSR) compact. This fact may be explained by assuming that the Al_4SiC_4(CVD/SSR) is more compositionally homogeneous and thermally stable compared to the Al_4SiC_4(CVD/SSR) compact.

Vickers hardness data for the hot-pressed Al_4SiC_4 (CVD/SSR) compacts have been shown in Fig. 8. It can be seen that the Vickers hardness value was ~13 GPa for hot pressing temperatures between 1700°C and 1900°C but decreased to 9 GPa for the temperature of 2000°C.

Although the relative densities of the Al_4SiC_4 (CVD/SSR) compacts hot-pressed at 1900°C and 2000°C for 1 h were similar (99.0%), the Vickers hardness was reduced considerably from 1900°C to 2000°C and attributed to thermal decomposition of the Al_4SiC_4. Thus, it is concluded that the optimum hot pressing temperature may be 1900°C. In addition, the amount of secondary phases appeared to be smaller compared to the case of the hot pressing temperature of 2000°C, although the XRD pattern has not been presented in this paper.

3.2.3. Thermal resistance of the Al_4SiC_4(CVD/SSR) compact

Since dense Al_4SiC_4(CVD/SSR) compacts with a relative density greater than 99.0% could be fabricated using the hot-pressing technique, the thermal resistance of these Al_4SiC_4(CVD/SSR) compacts was examined. The Al_4SiC_4(CVD/SSR) compact hot-pressed at 1900°C for 1 h was heat-treated at 1500°C for 1 h in air with the resulting TF-XRD pattern being shown in Fig. 9. The phases present were identified as Al_4SiC_4, mullite ($3Al_2O_3 \cdot 2SiO_2$ or $Al_6Si_2O_{13}$) [15], and α-Al_2O_3 [16].

The locations of the carbide and oxide compounds within the Al_4SiC_4 matrix were furthermore examined using EDX with results being shown in Fig. 10. The X-ray intensity attributed to AlKα was reduced, whereas that for SiKα was enhanced, with increasing depth from the surface to ~25 μm depth and then remained unchanged with further increases in depth from the surface.

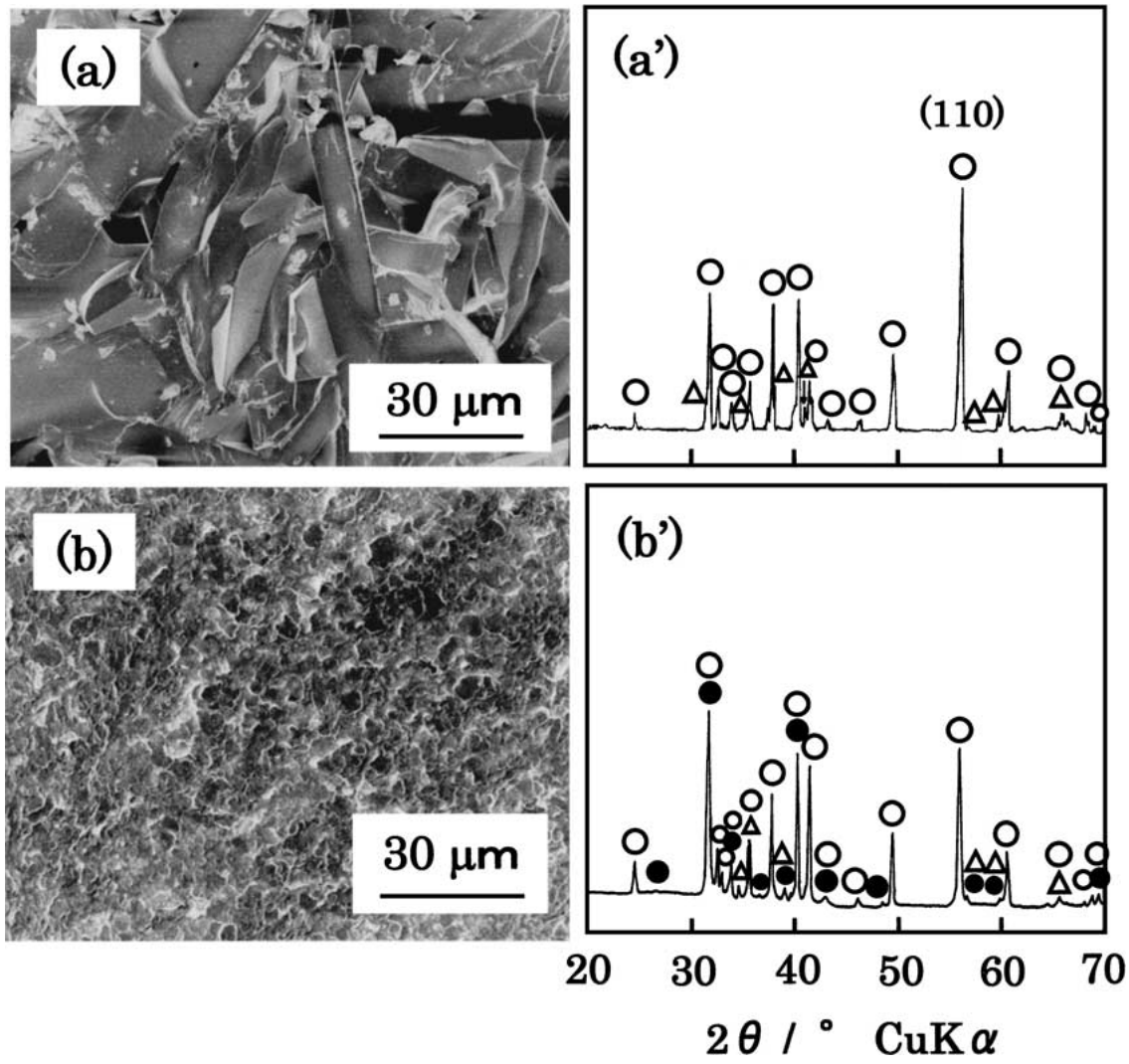

Figure 7 Typical SEM micrographs (left) and XRD patterns (right) for Al_4SiC_4(CVD/SSR) compacts pressureless-sintered and hot-pressed at 2000°C for 1 h. (a), (a'): Pressureless sintering (b), (b'): Hot pressing ○: Al_4SiC_4 ●: $Al_4Si_2C_5$ △: α-SiC.

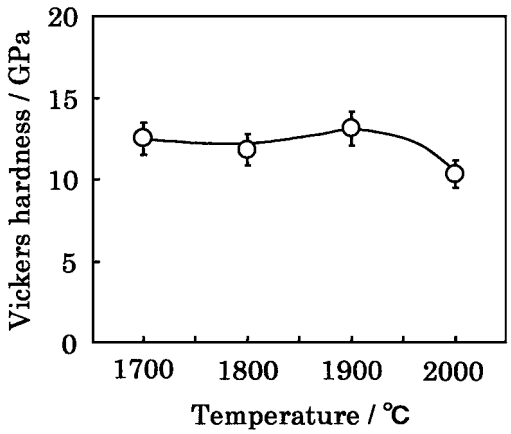

Figure 8 Effect of hot pressing temperature on the Vickers hardness of Al_4SiC_4(CVD/SSR) compact. Hot pressing time: 1 h.

In the early stage of oxidation, the reaction between Al_4SiC_4 and oxygen is reported to proceed as follows: [17]

$$Al_4SiC_4 + 6O_2 \rightarrow 2Al_2O_3 + SiC + 3CO_2 \qquad (4)$$

The resulting SiC reacts with oxygen to form silicon oxide (SiO_2) as follows:

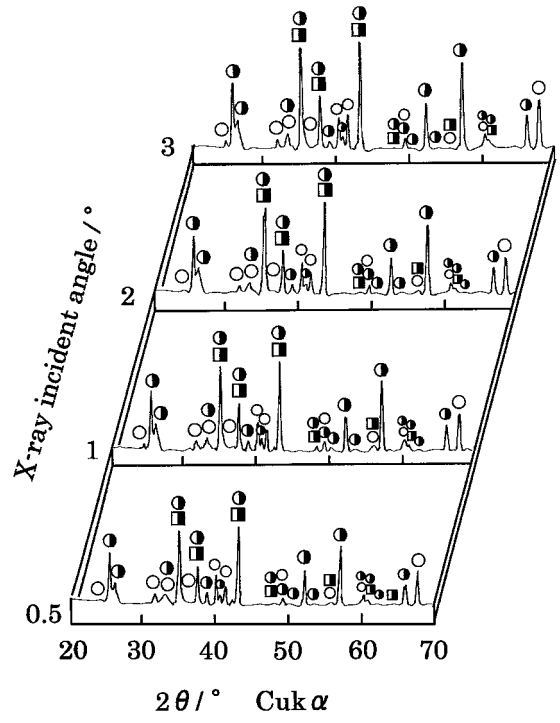

Figure 9 Typical TF-XRD patterns after the Al_4SiC_4(CVD/SSR) compact hot-pressed at 1900°C for 1 h was heat-treated at 1500°C for 1 h in air. ○: Al_4SiC_4 ◑: mullite ($3Al_2O_3 \cdot 2SiO_2$) ◨: Al_2O_3.

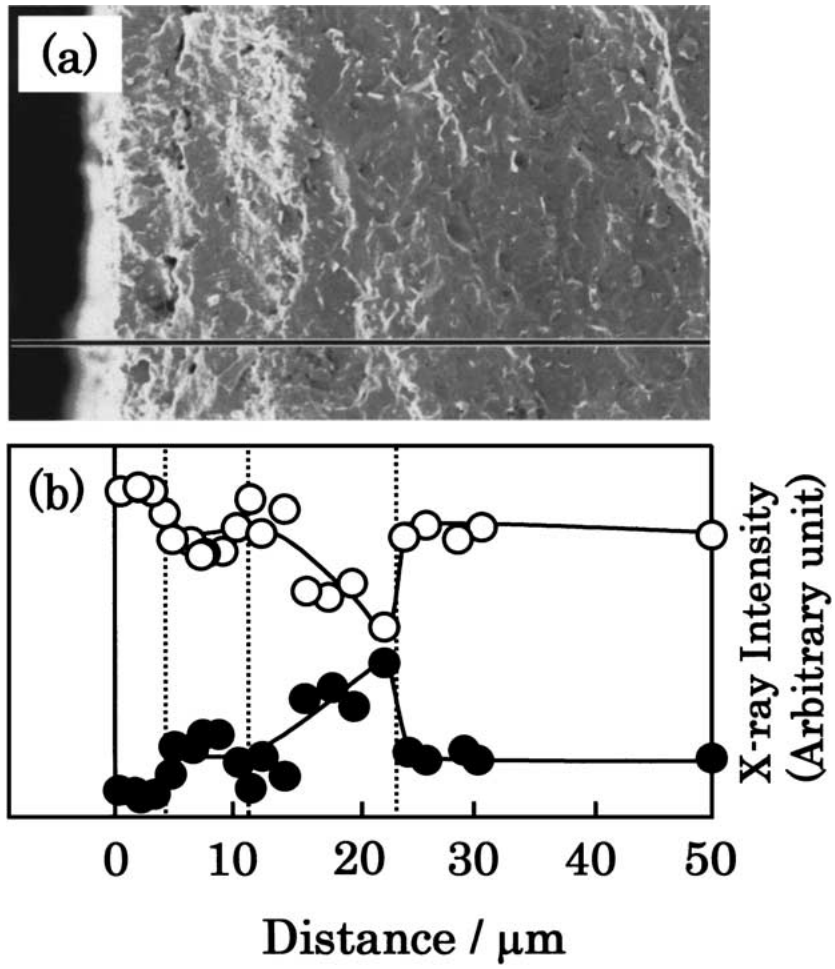

Figure 10 (a) SEM micrograph and (b) EDX results after the Al_4SiC_4(CVD/SSR) compact hot-pressed at 1900°C for 1 h was heat-treated at 1500°C for 1 h in air. ○–○: AlKα ●–●: SiKα. Note that the intensities of the AlKα and SiKα spectra on the horizontal line shown in the SEM micrograph were examined using EDX.

$$SiC + 2O_2 \rightarrow SiO_2 + CO_2 \quad (5)$$

Furthermore, Al_2O_3 reacts with SiO_2 to form mullite by the following route:

$$(3/2)Al_2O_3 + SiO_2 \rightarrow (1/2)Al_6Si_2O_{13} \quad (6)$$

According to Equations 4–6, one-half mole of Al_2O_3 does not participate in the formation of mullite, leaving excess Al_2O_3. On the basis of the TF-XRD and EDX data, therefore, the outer layer (thickness; ~5 μm) of heat-treated Al_4SiC_4(CVD/SSR) compact appeared to be Al_2O_3 with an inner layer of mullite (5–25 μm depth from the surface), and silicon oxide and carbide (10–25 μm depth from the surface).

The thickness of the oxides and carbides layers that covered the Al_4SiC_4 matrix was estimated to be approximately 25 μm. Note that these layers uniformly covered the Al_4SiC_4 matrix, contrary to an expectation that pores might be created due to the volume changes occurring during heating in air. The oxide layers are expected to inhibit further oxidation of the Al_4SiC_4. The authors are currently investigating some properties of the oxide layers and the results will be published at a later date.

4. Conclusions

Densification and microstructural developments during the sintering of aluminum silicon carbide (Al_4SiC_4) were examined. Two kinds of Al_4SiC_4 powders were prepared, namely by the solid-state reactions between: (i) Al, Si, and C at 1600°C for 10 h (Al_4SiC_4(SSR)), and (ii) chemically-vapour deposited ultrafine Al_4C_3 and SiC powders at 1500°C for 4 h (Al_4SiC_4(CVD/SSR)). The specific surface areas of the Al_4SiC_4(SSR) and Al_4SiC_4(CVD/SSR) powders were 2.7 and 15.5 $m^2 \cdot g^{-1}$, respectively. Dense Al_4SiC_4 ceramics were fabricated using these powders with the following results being obtained:

1. The relative densities of the pressureless-sintered Al_4SiC_4(SSR) and Al_4SiC_4(CVD/SSR) compacts were in the range 60–70% for a firing temperature between 1700°C and 2000°C. The relative density of the Al_4SiC_4(SSR) compact hot-pressed at 1900°C for 3 h was 97.0% whereas that of the Al_4SiC_4(CVD/SSR) compact hot-pressed at 1900°C for 1 h attained 99.0%. Densification of the Al_4SiC_4(CVD/SSR) compact appeared to be promoted, as a result of the higher surface area, reduced agglomeration of the primary particles, and more homogeneous chemical composition.

2. The grain morphologies for the hot-pressed Al_4SiC_4(SSR) compacts were significantly different

compared to those of the hot-pressed Al_4SiC_4 (CVD/SSR) compacts. The hot-pressed Al_4SiC_4(SSR) compacts were composed of plate-like grains of width 10–30 μm and thickness $\sim$10 μm, whereas the hot-pressed Al_4SiC_4(SSR) compact was comprised of equiaxed grains with diameters of typically $\sim$10 μm.

3. When the Al_4SiC_4(CVD/SSR) compact hot-pressed at 1900°C for 1 h was heat-treated at 1500°C for 1 h in air, the layers containing mullite ($3Al_2O_3 \cdot 2SiO_2$), α-Al_2O_3, and silicon oxide and carbide uniformly covered the Al_4SiC_4 matrix. The thickness of the layers was estimated to be approximately 25 μm.

Acknowledgements

The present authors wish to express their thanks to Mr. N. J. H. G. M. Lousberg of Eindhoven University of Technology (The Netherlands) for the WDX measurement.

References

1. V. J. BARCZAK, *J. Amer. Ceram. Soc.* **44** (1961) 299.
2. J. SCHOENNAHL, B. WILLER and M. DAIRE, "Material Science Monographs 4: Sintering - New Developments" (Elsevier Scientific Publishing, Amsterdam, The Netherlands, 1979) p. 338.
3. J. C. VIALA, P. FORTIER and J. BOIUIX, *J. Mater. Sci.* **25** (1990) 1842.
4. L. L. ODEN and R. A. MCCUNE, *Metall. Trans. A.* **18A** (1987) 2005.
5. H. YOKOKAWA, M. FUJISHIGE, S. UJIIE and M. DOKIYA, *Metall. Trans. B.* **18B** (1987) 433.
6. Z. INOUE, Y. INOMATA, H. TANAKA and H. KAWABATA, *J. Mater. Sci.* **15** (1980) 575.
7. K. ITATANI, M. HASEGAWA, M. AIZAWA, F. S. HOWELL, A. KISHIOKA and M. KINOSHITA, *J. Amer. Ceram. Soc.* **78** (1995) 801.
8. M. HASEGAWA, K. ITATANI, M. AIZAWA, F. S. HOWELL, A. KISHIOKA and M. KINOSHITA, *ibid.* **79** (1996) 275.
9. R. J. OSCROFT and D. P. THOMPSON, *ibid.* **75** (1992) 224.
10. R. RUH and A. ZANGVIL, *ibid.* **65** (1982) 260.
11. Joint Committee on Powder Diffraction Standards, No. 35-1072, JCPDS-International Centre for Diffraction Data, Newtown Square, PA (1985).
12. Joint Committee on Powder Diffraction Standards, No. 29-1131, JCPDS-International Centre for Diffraction Data, Newtown Square, PA (1972).
13. Joint Committee on Powder Diffraction Standards, No. 35-1073, JCPDS-International Centre for Diffraction Data, Newtown Square, PA (1985).
14. R. G. BEHRENS and G. H. RINEHART, *J. Amer. Ceram. Soc.* **67** (1984) 575.
15. Joint Committee on Powder Diffraction Standards, No. 15-776, JCPDS-International Centre for Diffraction Data, Newtown Square, PA (1965).
16. Joint Committee on Powder Diffraction Standards, No. 26-31, JCPDS-International Centre for Diffraction Data, Newtown Square, PA (1976).
17. YAMAGUCHI and S. ZHANG, *J. Ceram. Soc. Japan* **103** (1995) 20.

Received 12 October 2000
and accepted 1 September 2001